TÜBİTAK

Turkish Journal of Chemistry

http://journals.tubitak.gov.tr/chem/

Research Article

Turk J Chem
(2021) 45: 805-818
© TÜBİTAK
doi:10.3906/kim-2101-25

Novel Mannich bases with strong carbonic anhydrases and acetylcholinesterase inhibition effects: 3-(aminomethyl)-6-{3-[4-(trifluoromethyl)phenyl]acryloyl}-2(*3H*)-benzoxazolones

Sinan BiLGiNER[1,*], Barış ANIL[2], Mehmet KOCA[1], Yeliz DEMİR[3], İlhami GÜLÇİN[2]

[1]Department of Pharmaceutical Chemistry, Faculty of Pharmacy, Atatürk University, Erzurum, Turkey
[2]Department of Chemistry, Faculty of Science, Atatürk University, Erzurum, Turkey
[3]Nihat Delibalta Göle Vocational High School, Ardahan University, Ardahan, Turkey

Received: 11.01.2021 • **Accepted/Published Online:** 22.03.2021 • **Final Version:** 30.06.2021

Abstract: In this study, a new series of Mannich bases, 3-(aminomethyl)-6-{3-[4-(trifluoromethyl)phenyl]acryloyl}-2(*3H*)-benzoxazolones (**1a–g**), were synthesized by the Mannich reaction. Inhibitory effects of the newly synthesized compounds towards carbonic anhydrases (CAs) and acetylcholinesterase (AChE) enzymes were evaluated to find out new potential drug candidate compounds. According to the inhibitory activity results, K_i values of the compounds **1** and **1a–g** were in the range of 12.3 ± 1.2 to 154.0 ± 9.3 nM against hCA I, and they were in the range of 8.6 ± 1.9 to 41.0 ± 5.5 nM against hCA II. Ki values of acetazolamide (AZA) that was used as a reference compound were 84.4 ± 8.4 nM towards hCA I and 59.2 ± 4.8 nM towards hCA II. K_i values of the compounds **1** and **1a–g** were in the range of 35.2 ± 2.0 to 158.9 ± 33.5 nM towards AChE. K_i value of Tacrine (TAC), the reference compound, was 68.6 ± 3.8 nM towards AChE. Furthermore, docking studies were done with the most potent compounds **1d**, **1g**, and **1f** (in terms of hCA I, hCA II, and AChE inhibition effects, respectively) to determine the binding profiles of the series with these enzymes. Additionally, the prediction of ADME profiles of the compounds pointed out that the newly synthesized compounds had desirable physicochemical properties as lead compounds for further studies.

Key words: Acetylcholinesterase, carbonic anhydrase, chalcone, Mannich bases, molecular docking

1. Introduction

Alzheimer's disease (AD) is a devastating, multifactorial, chronic, and progressive neurodegenerative disease that causes dementia [1]. The fact that it is affecting 46.8 million people worldwide today indicates that AD is one of the most important health problems to be treated [2]. Although the disease cannot be cured, its progression can be stopped. According to the cholinergic hypothesis, which is one of the theses to understand the pathogenesis of the disease, losses occur both in the level of acetylcholine and cholinergic neurons in the cerebral cortex in AD [3–5]. For this purpose, many cholinesterase inhibitors such as donepezil, tacrine, and rivastigmine are used in the clinic. However, these drugs in the market have many side effects like nausea, diarrhea, hepatotoxicity, and vomiting [6]. Thus, there is a need for novel compounds having AChE inhibition effects with no or reduced side effects for the treatment of AD.

Carbonic anhydrases (CAs) are widespread zinc enzymes that are related to many important physiological and pathological processes via the hydration of carbon dioxide to bicarbonate [7,8]. To date, genetically eight different CA families have been determined as α-, β-, γ-, δ-, ζ- η-, θ-, and ι-CAs [9,10]. α-CA, which has 16 different isozymes, is involved in many different tissues and organs in mammals [11,12]. Thus, α-CA isoenzymes are used as drug targets in medicinal chemistry for the treatment of many diseases [12]. There are so many studies in the literature that report human carbonic anhydrase (hCA) inhibitors or activators with potential use as diuretic, anticancer, antiglaucoma, antiobesity, and antiinfective compounds [6,13–15]. Among hCAs, hCA I has an important function in the regulation of retinal edema [15,16]. Besides, hCA II isozyme inhibitor compounds are used in clinics as antiedema, antiglaucoma, and antiepileptic agents [4,12,15–18]. However, the hCA inhibitors used have undesired side effects because of having low selectivity to these isoenzymes [12,16–18]. As a result, there is a need in clinics for novel CA inhibitory compounds with higher inhibitory activity and selectivity to any of hCAs.

* Correspondence: sinanbilginer25@yahoo.com

The design of drugs bearing chalcones is often used in medicinal chemistry due to their several bioactivities such as antiinflammatory [19], antifungal [20,21], antimalarial [22,23], antimicrobial [24], anticancer [25,26], cytotoxic [10,27], antioxidant [28,29], carbonic anhydrase inhibiting [10,27,30], acetylcholinesterase inhibiting [31–34], and antidiabetic [35,36] activities. In our previous studies, we synthesized a series of benzoxazolone containing chalcone compounds and evaluated their cytotoxic and CA-inhibiting activities [27]. Among the series, trifluoromethyl derivative compound, 6-[3-(4-trifluoromethylphenyl)-2-propenoyl]-2(*3H*)-benzoxazolone (Figure 1), showed high inhibitory activities towards both hCA I and hCA II enzymes. For further studies, the previously synthesized chalcone compound presented in Figure 1 was planned to be derivatized from the 3rd position of the benzoxazolone ring by Mannich reaction.

Mannich bases are known as an important class in medicinal chemistry with various biological activities such as cytotoxic [25,37], antibacterial [38,39], antifungal [21,40], carbonic anhydrase inhibitory [41–44], and acetylcholinesterase inhibitory [42,45,46] activities. Moreover, Mannich bases are frequently used in drug design in medicinal chemistry because they alter the pharmacokinetic properties of compounds. The hydrophilic properties of compounds can be increased by adding a polar function to the structures of the compounds via aminomethylation (Mannich reaction) [47–49].

As conclusion, we first aimed to synthesize novel Mannich bases of the previously synthesized chalcone compound, 6-[3-(4-trifluoromethylphenyl)-2-propenoyl]-2(*3H*)-benzoxazolone, via aminomethylation from the 3rd position of the benzoxazolone ring. Carbonic anhydrase (CA) and acetylcholinesterase (AChE) inhibitory activities of the compounds were evaluated to find out new potential drug candidate molecule/s. Furthermore, docking studies were done to confirm and explain the inhibition effects of the newly synthesized compounds.

2. Materials and method

2.1. Chemistry

All chemicals and solvents were Sigma-Aldrich (Germany) and Merck (Germany). Bruker AVANCE III 400 MHz (Bruker, Karlsruhe, Germany) spectrometer [400 Hz (^{1}H) and 100 Hz (^{13}C)] was used to record the nuclear magnetic resonance (NMR) spectra (^{1}H NMR, ^{13}C NMR). Dimethyl sulfoxide (DMSO)-d6 was used as a solvent. NMR VTU technique was applied to keep the solubility of the compounds stable. The ^{1}H and ^{13}C NMR spectra of the compounds were recorded with dynamic NMR method at 328.15 K by using the Topspin 2.1 NMR program. The internal standard was tetramethylsilane. IR spectra of the compounds were recorded with the FTIR-ATR method (400–4000 cm^{-1}) on a IRSpirit Fourier transform (FT)-IR spectrophotometer (Shimadzu, Kyoto, Japan). Mass spectra of the samples were recorded using a liquid chromatography ion trap-time of flight tandem mass spectrometer (Shimadzu, Kyoto, Japan) equipped with an electrospray ionization (ESI) source, operating in both positive and negative ionization mode. For data analysis, Shimadzu's LCMS Solution program was used. Electrothermal 9100 instrument (IA9100, Bibby Scientific Limited, Staffordshire, UK) was used to determine the melting points of the compounds.

2.1.1. Synthesis of compound 1

The synthesis of the chalcone compound **1**, 6-[3-(4-trifluoromethylphenyl)-2-propenoyl]-2(*3H*)-benzoxazolone, was realized as described in detail in our previous study [27]. Briefly, 6-acetyl-2(*3H*)-benzoxazolone was synthesized by Friedel–Crafts reaction. Then, the chalcone compound **1** was synthesized by Claisen–Schmidt reaction that occurred between 6-acetyl-2(*3H*)-benzoxazolone and 4-trifluoromethyl benzaldehyde in basic condition as shown in Figure 2. 6-[3-(4-trifluoromethylphenyl)-2-propenoyl]-2(*3H*)-benzoxazolone was obtained with 80% yield. Physicochemical and spectroscopic characterizations of the compound **1** were reported in our previous study [27].

(*E*)-6-{3-[4-(trifluoromethyl)phenyl]acryloyl}benzoxazol-2(*3H*)-one (1)

White powder, yield 80%. Mp: 257–259 °C. IR (cm^{-1}) 1772, 1657, 1448, 1322, 1288, 1118, 1165, 1068, 815, 695. ^{1}H NMR (400 MHz, DMSO-d$_6$) δ (ppm) 8.12–8.14 (m, 3H, arom. H), 8.09 (d, 1H, Ar-CH=, *J* = 15.7 Hz), 8.06 (d, 1H, arom. H, *J* =

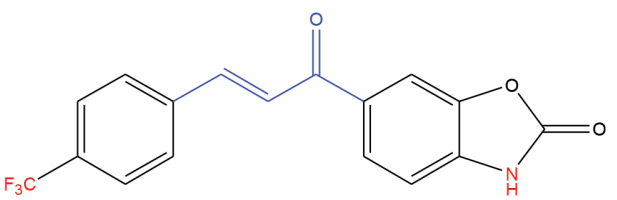

Figure 1. Structure of the previously synthesized compound showing high inhibitory activity towards both hCA I and hCA II enzymes.

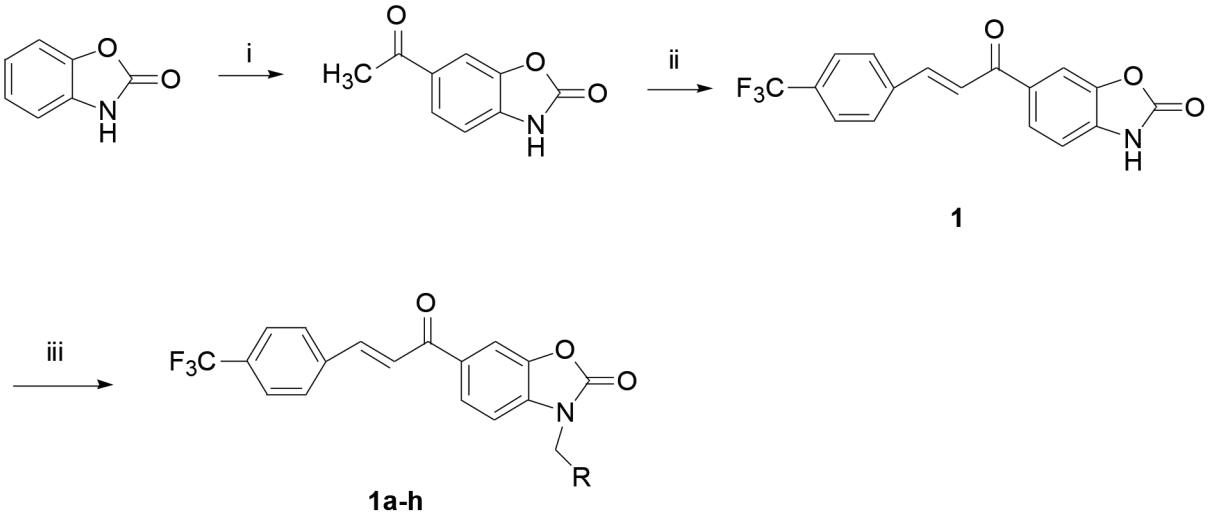

Figure 2. General synthetic pathway for compounds **1** and **1a – g.** Reagent and conditions: (i) CH_3COCl, $AlCl_3$-DMF; (ii) 4-trifluoromethylbenzaldehyde, aq. KOH, EtOH; (iii) suitable amine, 37% formaldehyde, EtOH **R**: Dimethylamino (**1a**), Diethylamino (**1b**), Dipropylamino (**1c**), Pyrrolidino (**1d**), Piperidino (**1e**), Morpholino (**1f**), and *N*-methyl piperazino (**1g**).

1.6 Hz), 7.80 (d, 2H, arom. H, *J* = 8.2 Hz), 7.78 (d, 1H, =CHCO, *J* = 15.7 Hz), 7.24 (d, 1H, arom. H, *J* = 8.2Hz). ^{13}C NMR (100 MHz, DMSO-d_6) δ (ppm) 187.7, 154.9, 143.9, 142.2, 139.2, 135.7, 131.9, 130.5, 129.9, 126.2, 124.9, 122.7, 119.1, 110.1. HRMS (ESI-MS) $C_{16}H_{11}NO_3$ m/z calculated $[M+H]^+$ 334.0686; measured 334.0687.

2.2.2. Synthesis of Mannich bases, 1a–g

To the solution of 6-[3-(4-trifluoromethylphenyl)-2-propenoyl]-2(*3H*)-benzoxazolone (0.1 g, 0.3 mmol) in ethanol (4 mL), 37% formaldehyde solution (33 µL, 0.4 mmol) was added and heated. Then, the suitable seconder amine compound (0.1 mmol) was added to this mixture and refluxed for 20 min (Figure 2). After standing at room temperature, the mixture was crystallized, filtered, washed with ethanol, dried [50] and recrystallized from ethanol.

3-[(Dimethylamino)methyl]-6-{3-[4-(trifluoromethyl)phenyl]acryloyl}benzoxazol-2(*3H*)-one (**1a**)

Yellow powder, yield 65%. Mp: 179–181 °C. IR (cm^{-1}) 1771, 1652, 1590, 1452, 1319, 1310, 1293, 1256, 1163, 1106, 1066, 926, 812, 694. ^{1}H NMR (400 MHz, DMSO-d_6) δ (ppm) 8.07 (4H, m, 4x Ar-CH), 8.02 (1H, d, *J* = 16.1 Hz, ol-CH), 7.76 (3H, m, 2xAr-CH, 1xol-CH), 7.44 (1H, bs, Ar-CH), 4.65 (2H, bs, N-CH_2-N), 2.33 (6H, bs, 2x CH_3). ^{13}C NMR (100 MHz, DMSO-d_6) δ (ppm) 187.76, 155.29, 144.31, 142.55, 136.89, 135.18, 132.75, 131.05, 129.39, 129.35, 128.71, 126.11, 122.23, 110.39, 110 02, 65.76, 42.70. HRMS (ESI-MS) $C_{20}H_{17}F_3N_2O_3$ m/z predicted $[M+H]^+$ 390.1191; found $[M+H]^+$ 390.1181.

3-[(Diethylamino)methyl]-6-{3-[4-(trifluoromethyl)phenyl]acryloyl}benzoxazol-2(*3H*)-one (**1b**)

Yellow powder, yield 72%. Mp: 235–236 °C. IR (cm^{-1}) 2977, 1762, 1668, 1618, 1324, 1269, 1121, 1068, 832, 608. ^{1}H NMR (400 MHz, DMSO-d_6) δ (ppm) 8.08 (2H, d, *J* = 8.0 Hz, Ar-CH), 8.04 (1H, d, *J* = 15.8 Hz, ol-CH), 7.92 (1H, s, Ar-CH), 7.78 (2H, d, *J* = 8.0 Hz, Ar-CH), 7.73 (1H, d, *J* = 15.8 Hz, ol-CH), 7.49 (1H, m, Ar-CH), 7.16 (1H, d, *J* = 6.89 Hz, Ar-CH), 4.75 (2H, s, N-CH_2-N), 2.66 (4H, q, *J* = 6.9 Hz, N-CH_2), 1.01 (6H, t, *J* = 7.0 Hz, 2x-CH_3). ^{13}C NMR (100 MHz, DMSO-d_6) δ (ppm) 187.85, 160.67, 142.38, 139.46, 130.14, 126.51, 126.38, 126.35, 126.30, 126.11, 125.19, 123.40, 110.71, 110.18, 86.88, 62.37, 45.13, 12.92. HRMS (ESI-MS) $C_{22}H_{21}F_3N_2O_3$ m/z predicted $[M+H]^+$ 418.1504; found $[M+H]^+$ 418.1490.

3-[(Dipropylamino)methyl]-6-{3-[4-(trifluoromethyl)phenyl]acryloyl}benzoxazol-2(*3H*)-one (**1c**)

Yellow powder, yield 37%. Mp: 157–158 °C. IR (cm^{-1}) 2966, 2923, 2355, 1772, 1653, 1559, 1456, 1325, 1068, 1033, 831. ^{1}H NMR (25 °C, 400 MHz, DMSO-d_6) δ (ppm) 8.10 (5H, m, 4x Ar-CH, 1x ol-CH), 7.78 (3H, m, 2x Ar-CH, 1x ol-CH), 7.41 (1H, d, *J* = 7.6 Hz, Ar-CH), 4.78 (2H, s, N-CH_2-N), 2.61 (t, 4H, *J* = 6.50 Hz, N-CH_2), 1.48 (m, 4H, 2x –CH_2-), 0.84 (t, 6H, *J* = 7.20 Hz, 2x CH_3). ^{13}C NMR (25 °C, 100 MHz, DMSO-d_6) δ (ppm) 187.74, 155.26, 142.85, 142.04, 139.29, 136.82, 132.39, 129.79, 126.23, 126.06, 126.02, 125.87, 125.23, 110.27, 109.94, 63.46, 53.87, 20.64, 11.92. HRMS (ESI-MS) $C_{24}H_{25}F_3N_2O_3$ m/z predicted $[M+H]^+$ 446.1817; found $[M+H]^+$ 446.1828.

3-(Pyrrolidin-1-ylmethyl)-6-{3-[4-(trifluoromethyl)phenyl]acryloyl}benzoxazol-2(*3H*)-one (**1d**)

Yellow powder, yield 85%. Mp: 179 °C. IR (cm^{-1}) 2973, 2821, 1772, 1656, 1592, 1455, 1321, 1165, 1106, 1067, 814, 694. ^{1}H NMR (400 MHz, DMSO-d_6) δ (ppm) 8.06 (5H, m, 4x Ar-CH, 1x ol-CH), 7.79 (2H, d, *J* = 8.9 Hz, 2xAr-CH), 7.73 (1H, s, Ar-CH), 7.54 (1H, bs, ol-CH), 4.84 (2H, s, N-CH_2-N), 2.51 (4H, bd, *J* = 1.3 Hz, N-CH_2-CH_2), 1.69 (4H, s, CH_2-CH_2). ^{13}C

NMR (100 MHz, DMSO-d_6) δ (ppm) 187.74, 153.35, 141.64, 139.39, 132.80, 129.73, 126.12, 126.07, 126.03, 126.01, 125.89, 125.45, 123,18, 110.15, 109.21, 65.21, 52.09, 22.31. HRMS (ESI-MS) $C_{22}H_{19}F_3N_2O_3$ m/z predicted $[M+H]^+$ 416.1348; found $[M+H]^+$ 416.1349.

3-(Piperidin-1-ylmethyl)-6-(3-(4-(trifluoromethyl)phenyl)acryloyl)benzoxazol-2(*3H*)-one (1e)

Yellow powder, yield 87%. Mp: 199–200 °C. IR (cm^{-1}) 2936, 1771, 1659, 1608, 1447, 1319, 1288, 1110, 1067, 811, 697. ^{1}H NMR (400 MHz, DMSO-d_6) δ (ppm) 8.08 (5H, m, 4x Ar-CH, 1x ol-CH), 8.02 (1H, s, Ar-CH), 7.77 (2H, m, 2x Ar-CH), 7.48 (1H, bs, ol-CH), 4.71 (2H, s, N-CH_2-N), 2.62 (4H, s, N-CH_2), 1.50 (4H, s, N-CH_2-CH_2), 1.34 (2H, s, -CH_2). ^{13}C NMR (100 MHz, DMSO-d_6) δ (ppm) 187.82, 155.31, 142.05, 139.27, 137.11, 132.41, 129.78, 126.22, 126.07, 126.03, 126.98, 125.86, 125.24, 110.39, 109.76, 65.73, 51.55, 25.83, 23.89. HRMS (ESI-MS) $C_{23}H_{21}F_3N_2O_3$ m/z predicted $[M+H]^+$ 430.1504; found $[M+H]^+$ 430.1495.

3-(Morpholinomethyl)-6-{3-[4-(trifluoromethyl)phenyl]acryloyl}benzoxazol-2(*3H*)-one (1f)

White powder, yield 89%. Mp: 215–217 °C. IR (cm^{-1}) 2865, 2833, 1768, 1656, 1449, 1324, 1111, 1068, 814, 695. ^{1}H NMR (400 MHz, DMSO-d_6) δ (ppm) 8.15 (1H, d, *J* = 15.2 Hz, ol-CH), 8.12 (2H, d, *J* = 8.8 Hz, 2x Ar-CH), 8.10 (2H, d, *J* = 8.6 Hz, 2x Ar-CH), 8.08 (1H, s, 1x Ar-CH), 7.79 (2H, m, Ar-CH, ol-CH), 7.55 (1H, d, *J* = 7.9 Hz, Ar-CH), 4.73 (2H, s, N-CH_2-N), 3.20 (4H, m, 2x -CH_2-O-), 2.66 (4H, m, 2x -CH_2-N-). ^{13}C NMR (100 MHz, DMSO-d_6) δ (ppm) 187.87, 155.09, 142.61, 142.18, 139.29, 136.74, 132.67, 129.83, 126.26, 126.09, 126.06, 125.27, 123.18, 110.42, 110.11, 66.49, 64.96, 50.73. HRMS (ESI-MS) $C_{22}H_{19}F_3N_2O_4$ m/z predicted $[M+H]^+$ 432.1297; found $[M+H]^+$ 432.1277.

3-[(4-Methylpiperazin-1-yl)methyl]-6-{3-[4-(trifluoromethyl)phenyl]acryloyl} benzoxazol-2(*3H*)-one (1g)

Yellow powder, yield 75%. Mp: 203–205 °C. IR (cm^{-1}) 2940, 2800, 1772, 1658, 1592, 1449, 1322, 1288, 1163, 1110, 1068, 815, 695. ^{1}H NMR (400 MHz, DMSO-d_6) δ (ppm) 8.09 (5H, m, 4x Ar-CH, 1x ol-CH), 7.80 (3H, m, 2x Ar-CH, 1x ol-CH), 7.41 (1H, d, *J* = 7.6 Hz, Ar-CH), 4.73 (2H, s, N-CH_2-N), 2.66 (4H, bs, 2x-N-CH_2), 2.32 (4H, bs, 2x-CH_2-N), 2.14 (3H bs, CH_3). ^{13}C NMR (100 MHz, DMSO-d_6) δ (ppm) 187.82, 155.05, 142.60, 142.11, 139.28, 136.79, 132.55, 129.80, 126.23, 126.07, 126.03, 125.26, 123.17,110.40, 110.05, 64.81, 54.88, 50.21, 46.03. HRMS (ESI-MS) $C_{23}H_{22}F3N_3O_3$ m/z predicted $[M+H]^+$ 445.1613; found $[M+H]^+$ 445.1604.

2.2. Acetylcholinesterase inhibition assay

Acetylcholinesterase enzyme inhibition assay was performed according to our previous studies [4,41,51–55]. The inhibition effects of the compounds **1** and **1a–g** on AChE enzyme, obtained from electric eel [56], were recorded in accordance with Ellman's method as demonstrated previously in detail [51,52,57]. The substrates of acetylthiocholine iodide (AChI) and 5,5'-dithiobis(2-nitro-benzoic acid) (DTNB) was used for cholinergic enzymatic reaction. For this purpose, 1 mL of Tris / HCl buffer (1.0 M, pH 8.0) and 10 µL of different concentrations of sample solution were dissolved in deionized water. Then, an aliquot of (50 µL) AChE enzyme was transferred and incubated at room temperature for 10 min. After the incubation period, an aliquot of DTNB (0.5 mM, 50 µL) was added. Then, the enzymatic reaction was started by adding 50 µL of AChI (10 mM). The breakdown of these substrates was monitored spectrophotometrically by the yellow color formation of 5-thio-2-nitrobenzoate anion as the result of the reaction of DTNB with thiocholine from hydrolysis of AChI with absorption at a wavelength of 412 nm [58,59].

2.3. Carbonic anhydrase inhibition assay

CA inhibition assay was recorded according to previous studies [4,10,27,49,60–64]. The hCA I and II isoenzymes were purified from human red blood cells by sepharose-4B-L-tyrosine-sulfanilamide affinity chromatography [65], which was used as an affinity matrix for selective retention of both hCA isoenzymes [27,66]. The inhibition effects of the compounds **1** and **1a–g** on both hCA isoenzymes were spectrophotometrically measured according to the previous method described in detail [49,60,67]. p-Nitrophenylacetate (PNA) was used as a substrate and changed to p-nitrophenolate ions (PNP). One CA isoenzyme unit is accepted as the amount of CA, which had absorbance change at 348 nm of PNA to PNP over a period of 3 min at 25 °C. After sepharose-4B-L-tyrosine-sulfanilamide affinity chromatography, the enzyme quantity was spectrophotometrically measured at 280 nm [68]. Moreover, the protein effluent was spectrophotometrically determined at 595 nm according to the Bradford method. Purity controls of both CA isoenzymes were performed according to the Laemmli procedure as described in previous studies. Both isoenzymes were visualized by two different acrylamide concentrations (10% and 3% acrylamide), containing 0.1% sodium dodecyl sulfate (SDS) [69,70].

2.4. Molecular docking studies

The most active compounds **1d** (pyrrolidine derivative) in terms of hCA I inhibition effect, **1g** (*N*-methyl piperazine derivative) in terms of hCA II inhibition effect, and **1f** (morpholine derivative) in terms of AChE inhibition effect were docked at the binding sites of the mentioned enzymes to describe and confirm the inhibition effects of the newly synthesized

compounds. The Protein Data Bank (PDB[1]) was used to get the structures of hCA I (4WR7), hCA II (3HS4), and AChE (1C2O) enzymes. The pdb files of the enzymes were prepared and transferred to AutoDockTools (ADT ver.1.5.6). Water molecules of the structures were removed and only polar hydrogen and Kollman charges were added to the proteins. Finally, the pdbqt files of the proteins were saved.

The Drug Bank[2] was used to get the chemical structures of the reference drugs (AZA and TAC). First, the active sites of the AChE and hCA I/II enzymes were defined by using BIOVIA Discovery Studio Visualizer (v20.1.0.19295). Then, the reference drugs, acetazolamide (AZA) and tacrine (TAC), were docked into the human carbonic anhydrases (hCA I/hCA II) and AChE, respectively. Compounds **1d**, **1g**, and **1f** were drawn in ChemDraw (Professional, Version 19.0.1.28), passed to ChemDraw 3D (Professional, Version 19.0.1.28), and minimized. The molecules' files were saved as pdb. Torsions of the compounds were examined and then compounds' files (**1d**, **1g**, and **1f)** were saved as pdbqt by AutoDockTools (ADT ver.1.5.6) [4].

AutoDockTools (ADT ver.1.5.6) was used for molecular docking studies. The Lamarckian genetic algorithm with local search (GALS) was used as a search engine, with a total of 10 runs. The active sites of enzymes were defined by a grid box of 70 × 70 × 70 points. Ten conformers of the compound were considered to evaluate the docking results. Finally, the conformer with the lowest binding free energy was evaluated using Python Molecule Viewer (PMV ver.1.5.6) and PyMOL (ver. 2.3.3, Schrodinger, LLC).

2.5. Estimation of physicochemical and ADME properties

In silico prediction of the ADME parameters and physicochemical properties the compounds was performed using the SwissADME[3] web tool. The structures of the compounds **1** and **1a–g** were drawn and transformed to SMILES (simplified molecular-input line-entry system). Finally, the ADME parameters and physicochemical parameters of the compounds **1** and **1a–g** were calculated by running the program.

3. Results and discussion

3.1. Chemistry

The compounds **1** and **1a–g** were synthesized successfully for the first time (except **1** and **1g**) [27,71] according to Figure 2. First, the chalcone compound **1**, 6-[3-(4-trifluoromethylphenyl)-2-propenoyl]-2(*3H*)-benzoxazolone, was synthesized according to our previous study [27] by the classical Claisen-Schmidt reaction realized between 4-trifluorobenzaldehyde and 6-acetyl-2(*3H*)-benzoxazolone [10,27]. In the second step, the Mannich bases were synthesized by the Mannnich reaction of compound **1** with suitable seconder amines. The amine compounds used were as follows: dimethylamine (**1a**), diethylamine (**1b**), dipropylamine (**1c**), pyrrolidine (**1d**), piperidine (**1e**), morpholine (**1f**), and 1-methyl piperazine (**1g**). The compound synthesized with the highest yield was morpholine derivative compound **1f** (89%) while the compound synthesized with the lowest yield was dipropylamine derivative compound **1c** (37%) in the series.

According to IR spectra of the compounds, the lactam and ketone C=O stretching bands were seen about 1770 cm^{-1} and 1650 cm^{-1}. According to ^{1}H NMR spectra of the synthesized compounds**,** the methylene protons between two nitrogen atoms of Mannich bases appeared at the area of 4.5–5.5 ppm as expected. On the other hand, ^{1}H NMR spectra of the compounds showed that all compounds were configured *trans*, as understood from coupling constant J = 15.2 – 16.1 Hz for vinyl protons or from the results of the NOESY NMR of the compounds. The DEPT NMR spectra of the compound **1a** were recorded to determine primary, secondary, and tertiary carbon atoms of the series. According to the DEPT NMR results of the compound **1a**, carbons of the carbonyl groups were seen about 187 ppm (ketone) and 155 ppm (lactam). Signals of the other quaternary carbons were seen at 142.55, 136.89, 135.18, 132.75, 128.71, and 110.02 ppm. In the aliphatic region, the carbon of methylene group (secondary) was seen as a negative signal while the carbons of methyl groups (primary) were seen as a positive signal. The chemical structures of the newly synthesized compounds **1, 1a–g** were confirmed and characterized by IR, ^{1}H NMR, ^{13}C NMR, and HRMS (see the experimental part for details).

3.2. Carbonic anhydrases inhibitory activities

The CA inhibition effects of the compounds **1a–g** were reported for the first time in this study, and the CA inhibition results are shown in Table 1. Acetazolamide (AZA) was used as a reference drug, and its K_i values were 84.4 ± 8.4 nM towards hCA I and 59.2 ± 4.8 nM towards hCA II.

The compounds **1** and **1a–g** had K_i values of in the range of 12.3 ± 1.2 to 154.0 ± 9.3 nM towards hCA I (Table 1). According to hCA I inhibitory activity results of the compounds, all Mannich bases synthesized (**1a–g)** had higher

[1] https://www.rcsb.org/

[2] https://www.drugbank.ca/

[3] http://www.swissadme.ch/

Table 1. Inhibition effects of the compounds **1** and **1a–g** on hCA I, hCAII, and AChE enzymes.

Compounds	K_i (nM)		
	hCA I*	hCA II*	AChE*
1	154.0 ± 9.3	33.6 ± 4.5	158.9 ± 33.5
1a	31.4 ± 5.3	23.3 ± 2.0	129.9 ± 17.6
1b	36.8 ± 7.7	37.6 ± 4.3	142.1 ± 22.1
1c	22.3 ± 2.3	24.6 ± 4.7	115.8 ± 32.0
1d	12.3 ± 1.2	19.0 ± 3.0	97.6 ± 14.4
1e	27.6 ± 2.9	18.1 ± 3.5	84.0 ± 19.2
1f	20.4 ± 1.7	41.0 ± 5.5	35.2 ± 2.0
1g	53.0 ± 1.8	8.6 ± 1.9	48.5 ± 10.2
AZA**	84.4 ± 8.4	59.2 ± 4.8	-
TAC***	-	-	68.6 ± 3.8

* Mean from three different assays.
**Acetazolamide (AZA) was used as a standard inhibitor for both hCA I and II isoenzymes.
***Tacrine (TAC) was used as a standard inhibitor for AChE enzyme.

inhibitory activities than the reference compound, AZA. On the other hand, compound **1** had both the lowest inhibitory activity in the series and lower inhibitory activity than the reference compound, AZA. As a result, the aminomethylation from the 3rd position of the benzoxazolone ring by Mannich reaction caused a significant increase (in the range of 2.1–12.5 times) in hCA I inhibition effects, as expected. This result suggested that the prevention of tautomerization between the nitrogen atom and carbonyl of the benzoxazolone ring had a crucial role in hCA I inhibitory activity. According to the K_i values presented in Table 1, the pyrrolidine derivative compound **1d** had the highest inhibition effect in the series with a lower K_i value (12.3 ± 1.2 nM) than AZA (K_i = 84.4 ± 8.4 nM) towards hCA I. Including the nitrogen atom of Mannich base in a cyclic structure (pyrrolidine derivative compound **1d**) led to an approximately three-fold increase in hCA I inhibitory activity comparing to diethylamine derivative compound **1b**. On the other hand, replacing the pyrrolidine ring (compound **1d**) with a six-membered ring (piperidine derivative compound **1e**) led to an approximately two-fold decrease in hCA I inhibitory activity. Comparing the K_i values of compounds **1e** and **1f** pointed out that the replacement of the carbon atom on the piperidine heterocycle with the oxygen atom caused an increase in the hCA I inhibition effect. This may be due to the formation of a hydrogen bond between the oxygen atom and the active site of hCA I isoenzyme.

According to Table 1, K_i values of the compounds **1, 1a–g** were in the range of 8.6 ± 1.9 to 41.0 ± 5.5 nM towards hCA II isoenzyme. The hCA II inhibitory activity results of the compounds presented in Table 1 showed that all compounds synthesized (**1** and **1a–g**) showed higher inhibition effects with their lower K_i values than the reference compound AZA. Thus, the results presented in Table 1 pointed out that the aminomethylation from the 3rd position of the benzoxazolone ring by Mannich reaction generally resulted in an increase (except compounds **1b** and **1f**) in hCA II inhibitory activity. The most potent compound in the series was *N*-methyl piperazine derivative compound **1g** with the remarkable K_i value of 8.6 ± 1.9 nM, which is approximately 7 times lower than AZA. Thus, compound **1g** was the most important compound of the series in terms of hCA II inhibitory activity and can be regarded as a lead molecule for further investigations. According to Table 1, the morpholine derivative compound **1f** had the lowest hCA II inhibition effect in the series with the K_i value of 41.0 ± 5.5 nM which is 1.4 times lower than AZA. The pyrrolidine derivative compound **1d** including the nitrogen atom of Mannich base in a cyclic structure had higher inhibitory activity (K_i = 19.01 ± 3.0 nM) about 2 times towards hCA I than diethylamine derivative compound **1b** (K_i = 37.6 ± 4.3 nM). Comparing the K_i values of compounds **1e** and **1f** towards hCA II showed that the replacement of the carbon atom on the piperidine heterocycle with the oxygen atom led to a decrease about 2 times in the hCA II inhibition effect. On the other hand, the inhibition results in Table 1 suggested that the compounds carrying the nitrogen atom of Mannich base in a cyclic structure (compounds **1d - g**) generally had higher inhibitory activities towards hCA II isoenzyme than the compounds carrying the nitrogen atom of Mannich bases on a straight chain (compounds **1a–c**).

Table 2. Docking results of the compounds **1**, **1d**, **1g**, and **1f**.

	hCA I		hCA II		AChE	
Compound	Energy scrore	Ki (μM)	Energy scrore	Ki (μM)	Energy scrore	Ki (nM)
1	–6.62	14.01	–7.43	3.6	–8.82	342.12
1d	–8.18	1.01	-	-		
1g	-	-	–8.05	1.25	-	-
1f	-	-			–10.17	35.38
AZA*	–6.53	16.39	–6.77	10.97		
TAC**	-	-	-	-	–7.1	6.3 μM

*Acetazolamide (AZA) was used as a reference compound for both hCA I (4WR7) and hCA II (3HS4).
**Tacrine (TAC) was used as a reference compound for AChE (1C2O).

3.3. AChE inhibitory activities

The AChE inhibitory activities of the newly synthesized compounds **1** and **1a–g** were reported for the first time in this study and the results were presented in Table 1. The reference drug used was tacrine (TAC) and its K_i value was 68.6 ± 3.8 nM towards AChE enzyme. According to the results presented in Table 1, K_i values of the compounds **1** and **1a–g** were in the range of 35.2 ± 2.0 to 158.9 ± 33.5 nM towards AChE. The inhibition results showed that compounds **1f** and **1g** had higher inhibitory effects than the reference drug TAC. The morpholine derivative compound **1f** was the most active compound in the series with the K_i value as 35.2 ± 2.0 nM. On the other hand, the chalcone compound **1** had the lowest inhibition effect in the series with the K_i value as 158.9 ± 33.5 nM. Thus, the inhibition results showed that synthesis of Mannich derivatives from the 3rd position of the benzoxazole ring of the compound **1** was a modification that contributed to the AChE inhibition effect. This may be due to the prevention of tautomerization between the amino and carbonyl groups of the benzoxazolone ring. Besides, the inhibition results presented in Table 1 pointed out that the compounds where the nitrogen atom of Mannich base was included in a cyclic structure (compounds **1d - g**) had higher inhibitory effects on AChE enzyme than the compounds carrying the nitrogen atom of Mannich bases on a straight chain (compounds **1a–c**). Even, adding one more heteroatom (oxygen or nitrogen) to this heterocyclic structure (compounds **1f** and **1g**, respectively) resulted in an increase in AChE inhibitory activity comparing to piperidine derivative compound **1e**.

3.4. Molecular docking studies

To demonstrate the binding model of the synthesized compounds **1** and **1a–g** with the active sites of hCA I, hCA II, and AChE enzymes, docking studies were performed using AutoDockTools (ADT ver.1.5.6). The X-ray crystallographic structures of hCA I (4WR7), hCA II (3HS4), and AChE (1C2O) were obtained from the Protein Data Bank[4]. The chalcone compound **1** and the most potent compounds **1d** (pyrrolidine derivative), **1g** (*N*-methyl piperazine derivative), and **1f** (morpholine derivative) in terms of hCA I, hCA II, and AChE inhibitory activities (respectively) were docked at the binding sites of the mentioned enzymes to describe and confirm the inhibition effects of the series.

First, the active sites of the hCA I, hCA II, and AChE were defined by using BIOVIA Discovery Studio Visualizer. Then, the reference drugs acetazolamide (AZA) and tacrine (TAC) were docked into the human carbonic anhydrases (hCA I and hCA II) and AChE, respectively. These simulations were done successfully and the binding free energy scores of the reference drugs were found as –6.53 (in 4WR7), –6.77 (in 3HS4), and –7.10 (in 1C2O) kcal / mol. Finally, the binding free energy scores and K_i values of the chalcone compound **1** and the most potent compounds **1d**, **1g**, and **1f** in the series were calculated by docking simulations and the results were presented in Table 2.

The energy score of the most active compound **1d** (pyrrolidine derivative) towards hCA I was found as –8.18 kcal/mol. Thus, this suggested the strong interactions of the compound with the active site of the 4WR7, as expected. According to Figure 3, the carbonyl moiety of the benzoxazolone ring of the compound **1d** realized a hydrogen bonding with the amino groups of the amino acids His200. This showed the importance of the prevention of tautomerization between the nitrogen atom and carbonyl of the benzoxazolone ring by Mannich reaction in designing hCA I inhibitory compounds in terms of the strong interactions with the enzyme. Besides, the pyrrolidine ring realized a hydrophobic interaction with the amino acid Thr199. According to the binding pattern of compound **1d** presented in Figure 3, the π-cation interaction was exhibited between the benzoxazolone ring of the compound and the side chain of the amino acid His200. On the other

[4] https://www.rcsb.org/

hand, seven hydrophobic interactions were exhibited between the compound **1d** and the amino acids Phe91, His119, Leu131, Val143, Leu198, and Trp209. Furthermore, trifluoromethyl moiety of the compound **1d** involved in a halogen bond with the amino acid Phe91. This pointed out that the trifluoromethyl group of the compounds designed had an important role in strong interactions with the active site of the hCA I isoenzyme, as planned.

Compound **1g**, *N*-methyl piperazine derivative, showed higher inhibitory activity (K_i = 8.6 ± 1.9 nM) than AZA towards hCA II and its docking score was –8.05 kcal/mol that is lower than the reference drug's binding free energy (–6.77

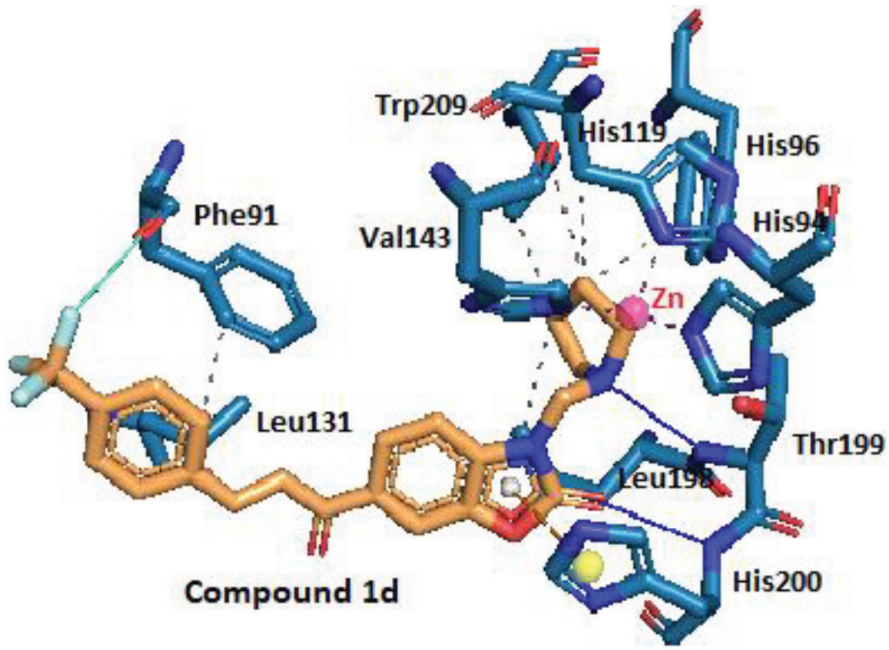

Figure 3. Three-dimensional representation of compound **1d**, showing its interaction with the active site of hCA I. Grey color represents hydrophobic interactions, blue color represents hydrogen bondings, green color represents halogen bonds, and red represents π-cation interactions.

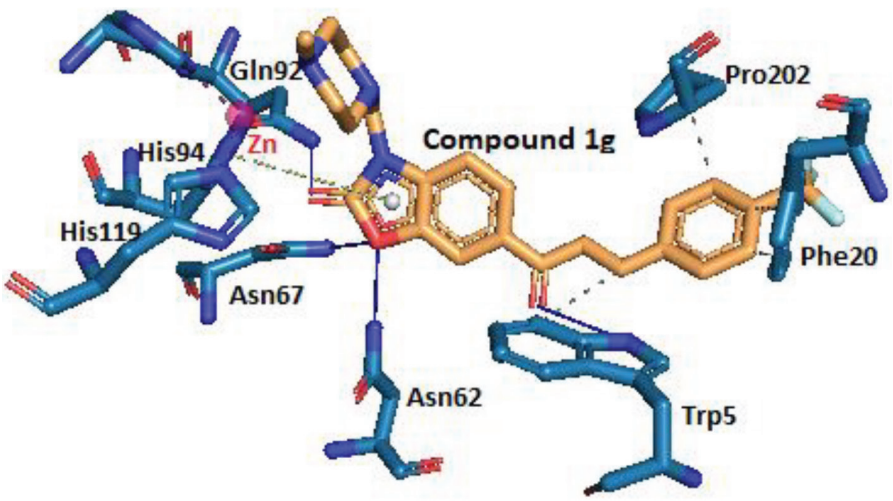

Figure 4. Three-dimensional representation of compound **1g**, showing its interaction with the active site of hCA II. Grey color represents hydrophobic interactions, blue color represents hydrogen bondings, and green represents π-stacking interactions.

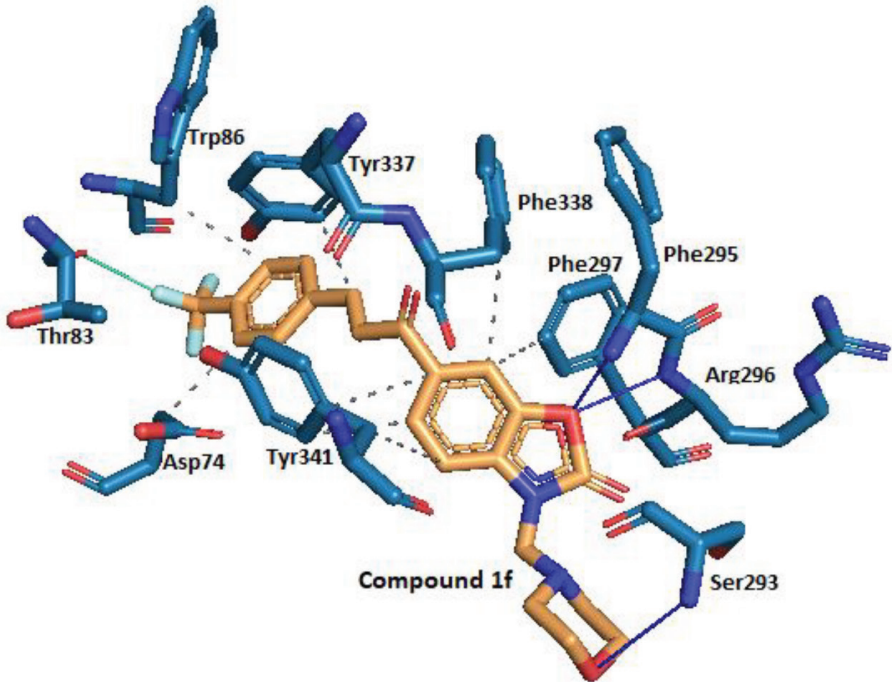

Figure 5. Three-dimensional representation of compound **1f**, showing its interaction with the active site of AChE. Grey color represents hydrophobic interactions, blue color represents hydrogen bondings, and the green represents halogen bonds.

kcal/mol), as expected. The binding pattern of compound **1g** with the active site of the hCA II enzyme (3HS4) is shown in Figure 4. In Figure 4, it was seen that the carbonyl group of benzoxazolone heterocycle of compound **1g** realized a hydrogen bond with the side chain of the amino acid Gln92. This shows how the prevention of tautomerization between amino and carbonyl groups by aminomethylation contributes positively to hCA II inhibitory activity. Furthermore, two hydrogen bonds were observed between the oxygen atom of the benzoxazolone ring and the amino acids Asn62 and Asn67. On the other hand, the carbonyl group of chalcone structure of compound **1g** realized a hydrogen bond with the side chain of the amino acid Trp5. According to the binding profile of compound **1g** (Figure 4), π-stacking interaction was exhibited between the benzoxazolone ring of the compound and the amino acid His94. Besides, four hydrophobic interactions were seen between the compound **1g** and the amino acids Trp5, Phe20, and Pro202.

The morpholine derivative compound **1f** had the highest inhibition effect on AChE enzyme in the series and docked in 1C2O to explain its inhibition effect. As expected, compound **1f** had lower energy score, –10.17 kcal/mol, in AChE than reference drug TAC (–7.10 kcal/mol), recommending a strong interaction between the compound **1f** and the 1C2O. According to Figure 5, the oxygen atom on the first position of the benzoxazolone ring interacted with the enzyme via two hydrogen bonds with the amino groups of the amino acids Phe295 and Arg296. Similarly, the oxygen atom of the morpholine moiety formed a hydrogen bond with the amino group of Ser293. Thus, this suggested that aminomethylation of benzoxazolone ring with morpholine was a useful modification in terms of strong interactions with the active site of AChE. On the other hand, eight hydrophobic interactions were detected between compound **1f** and the amino acids Asp74, Trp86, Phe297, Tyr337, Phe338, and Tyr341 (Figure 5). Additionally, one halogen bond was exhibited between the trifluoromethyl group of the compound **1f** and the side chain of the amino acid Thr83. This pointed out the importance of the trifluoromethyl moiety in designing in terms of AChE inhibition effect.

3.5. Estimation of physicochemical properties

Both the physicochemical and the ADME properties of a compound are very crucial in oral drug-candidate designing. 'Drug-likeness' is a term that describes the potentiality for a compound to be an oral drug in terms of bioavailability [72]. Lipinski's 5 rules are used to evaluate this potentiality of a molecule [4,73]. In this study, both the physicochemical and the pharmacokinetic properties of the synthesized compounds **1** and **1a–g** were estimated using the SwissADME[5] web tool [4,72]. For this purpose, molecular weights, the numbers of hydrogen bond acceptors and donors, the topological surface

[5] http://www.swissadme.ch/index.php

Table 3. In silico physicochemical and pharmacokinetic properties of the compounds **1** and **1a – g**.

Compound	MW[a]	HBA[b]	HBD[c]	TPSA[d]	$CLogP_{o/w}$[e]	logS[f]	Bioavailability score[g]
1	333.26	6	1	63.07	3.88	- 4.49	0.55
1a	390.36	7	0	55.45	3.97	- 4.85	0.55
1b	418.41	7	0	55.45	4.57	- 5.33	0.55
1c	446.46	7	0	55.45	5.29	- 6.01	0.55
1d	416.39	7	0	55.45	4.28	- 5.29	0.55
1e	430.42	7	0	55.45	4.57	- 5.59	0.55
1f	432.39	8	0	64.68	3.70	- 4.83	0.55
1g	445.43	8	0	58.69	3.75	- 5.02	0.55

[a] Molecular weight (<500 Da), [b] Number of hydrogen bond acceptors (<10), [c] Number of hydrogen bond donors (<5), [d] Topological polar surface area (20–130 Å^2), [e] Octanol/water partition coefficient (Consensus logP value, recommended range: −2.0 to 6.5), [f] Aqueous solubility prediction (not higher than 6), [g] Abbott bioavailability score (probability at least 10% oral bioavailability in rat).

areas (TPSA; a sum of polar atoms' surfaces), lipophilicities, water solubilities, and bioavailability of the synthesized compounds **1** and **1a–g** are presented in Table 3.

The results in Table 3 showed that all of the synthesized compounds were in agreement with Lipinski's rule of 5. The compounds' ClogP values ranged between 3.70 and 5.29 (<6.5), molecular weight range of 333.26–446.26 (<500), HBA range of 6–8 (≤ 10), and HBD values 0–1 (<5), suggesting that compounds **1** and **1a–g** have desired drug-likeness properties. On the other hand, all of the compounds had desired logP values and were estimated to have high gastrointestinal absorption and to penetrate the blood-brain barrier. These are advantages for the oral use of the synthesized compounds as AChE inhibitors in AD.

The radar charts of the most potent compounds **1d, 1g,** and **1f** towards hCA I, hCA II, and AChE, respectively, are shown in Figure 6. The pink-colored areas in these charts demonstrate the ideal ranges for each physicochemical properties; LIPO (lipophilicity, XLogP: between –0.7 and +5.0), size (MW: between 150 and 500 g/mol), POLAR (polarity, TPSA: between 20 and 130 Å^2), INSOLU (solubility, log S: not higher than 6), INSATU (saturation; the fraction of carbons in the sp^3 hybridization not less than 0.25), FLEX (flexibility, no more than 9 rotatable bonds) [72]. The radar charts presented in Figure 6 pointed out that the physicochemical properties of the most potent compounds **1d**, **1g**, and **1f** were fully located in the pink-colored area. As a result, the leading compounds **1d**, **1g**, and **1f** of the series were predicted as oral bioavailable drug candidates due to having promising pharmacokinetic properties.

4. Conclusion

The designed compounds **1a–g**, 3-(aminomethyl)-6-{3-[4-(trifluoromethyl)phenyl]acryloyl}-2(*3H*)-benzoxazolones, were synthesized and purified successfully. Their inhibition effects on hCA I, hCA II, and AChE enzymes were investigated for the first time. The inhibition results of the newly synthesized compounds showed that all Mannich bases had higher inhibitory activities against carbonic anhydrases (hCA I and hCA II) than the reference compound AZA. The pyrrolidine derivative compound **1d** had the highest inhibition effect in the series on hCA I with a lower K_i value (12.3 ± 1.2 nM) than AZA (K_i = 84.4 ± 8.4 nM). Besides, the most potent compound in the series was the *N*-methyl piperazine derivative compound **1g** having K_i value as 8.55 ± 1.90 nM towards hCA II. According to the hCA inhibition results, compounds **1d** and **1g** were the most expressive lead compounds of the study with remarkable K_i values (12.3 nM and 8.55 nM, respectively) which are approximately 7 times lower than AZA. According to the AChE inhibitory activity results, the morpholine derivative compound **1f** was the most active compound in the series with the K_i value as 35.2 ± 2.0 nM, which is about two-fold lower than the reference drug, TAC. On the other hand, the most active compounds **1d** (pyrrolidine derivative) towards hCA I, **1g** (*N*-methyl piperazine derivative) towards hCA II, and **1f** (morpholine derivative) towards AChE were docked at the binding sites of the mentioned enzymes to explain the inhibitory activities of the compounds. The docking results showed that the compounds **1d**, **1g**, and **1f** had strong interactions with the active sites of hCA I, hCA II, and AChE, as expected. ADME prediction studies of the compounds **1** and **1a–g** pointed out that the newly synthesized Mannich bases were not only potent AChE and CAs inhibitory compounds but also had promising physicochemical

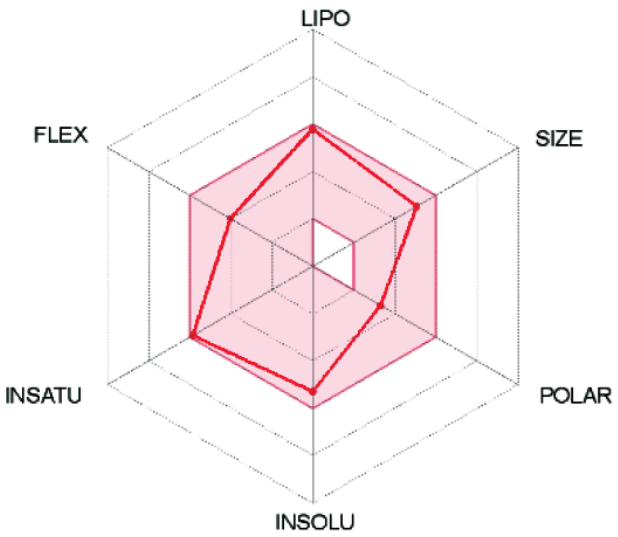

Compound 1d

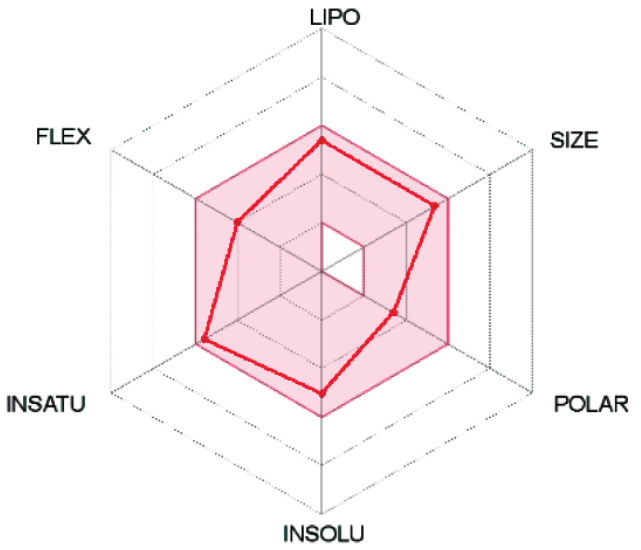

Compound 1g

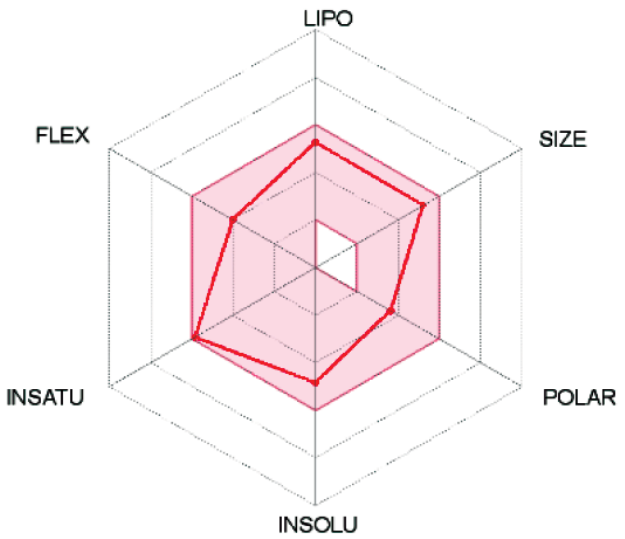

Compound 1f

Figure 6. Bioavailability radar charts of compounds **1d**, **1g**, and **1f**.

and ADME properties for further investigations. As a conclusion, in vitro inhibition results and in silico studies of the synthesized compounds showed that the aminomethylation from the 3rd position of the benzoxazolone ring of the chalcone compound **1** by Mannich reaction is a useful modification in terms of carbonic anhydrases and AChE inhibitory activities as well as optimization of physicochemical and pharmacokinetic properties.

References

1. Akıncıoğlu H, Gülçin İ. Potent acetylcholinesterase inhibitors: Potential drugs for Alzheimer's disease. Mini Reviews in Medicinal Chemistry. 2020; 20 (8): 703-715.

2. Nguyen KV. Special Issue: Alzheimer's disease. AIMS Neuroscience 2018; 5 (1): 74-80.

3. Aktas A, Barut Celepci D, Gok Y, Taslimi P, Akincioglu H et al. A novel ag-n-heterocyclic carbene complex bearing the hydroxyethyl ligand: synthesis, characterization, crystal and spectral structures and bioactivity properties. Crystals 2020; 10 (3): 171.

4. Bilginer S, Gul HI, Anil B, Demir Y, Gulcin I. Synthesis and in silico studies of triazene-substituted sulfamerazine derivatives as acetylcholinesterase and carbonic anhydrases inhibitors. Archiv der Pharmazie.e2000243.

5. Craig LA, Hong NS, McDonald RJ. Revisiting the cholinergic hypothesis in the development of Alzheimer's disease. Neuroscience & Biobehavioral Reviews 2011; 35 (6): 1397-1409.

6. Günsel A, Bilgiçli AT, Barut B, Taslimi P, Özel A et al. Synthesis of water soluble tetra-substituted phthalocyanines: investigation of DNA cleavage, cytotoxic effects and metabolic enzyme inhibition. Journal of Molecular Structure 2020: 128210.

7. Bilgiçli HG, Ergön D, Taslimi P, Tüzün B, Kuru İA et al. Novel Propanolamine derivatives attached to 2-metoxifenol moiety: synthesis, characterization, biological properties, and molecular docking studies. Bioorganic Chemistry 2020: 103969.

8. Supuran CT. Carbonic anhydrases-an overview. Current Pharmaceutical Design 2008; 14 (7): 603-614.

9. Artunc T, Menzek A, Taslimi P, Gulcin I, Kazaz C et al. Synthesis and antioxidant activities of phenol derivatives from 1, 6-bis (dimethoxyphenyl) hexane-1, 6-dione. Bioorganic Chemistry 2020: 103884.

10. Bilginer S, Gul HI, Erdal FS, Sakagami H, Gulcin I. New halogenated chalcones with cytotoxic and carbonic anhydrase inhibitory properties: 6-(3-Halogenated phenyl-2-propen-1-oyl)-2 (3H)-benzoxazolones. Archiv der Pharmazie 2020; 353 (6): 1900384.

11. Caglayan C, Taslimi P, Türk C, Gulcin I, Kandemir FM et al. Inhibition effects of some pesticides and heavy metals on carbonic anhydrase enzyme activity purified from horse mackerel (Trachurus trachurus) gill tissues. Environmental Science and Pollution Research 2020: 1-10.

12. Supuran CT. Carbonic anhydrase inhibitors and activators for novel therapeutic applications. Future Medicinal Chemistry 2011; 3 (9): 1165-1180.

13. Alterio V, Di Fiore A, D'Ambrosio K, Supuran CT, De Simone G. Multiple binding modes of inhibitors to carbonic anhydrases: how to design specific drugs targeting 15 different isoforms? Chemical Reviews 2012; 112 (8): 4421-4468.

14. Taslimi P, Turhan K, Türkan F, Karaman HS, Turgut Z et al. Cholinesterases, α-glycosidase, and carbonic anhydrase inhibition properties of 1H-pyrazolo [1, 2-b] phthalazine-5, 10-dione derivatives: Synthetic analogues for the treatment of Alzheimer's disease and diabetes mellitus. Bioorganic Chemistry 2020; 97: 103647.

15. Supuran CT, Scozzafava A, Conway J. Carbonic anhydrase: its inhibitors and activators: CRC press; 2004.

16. Supuran CT, Scozzafava A. Carbonic anhydrase inhibitors and their therapeutic potential. Expert Opinion on Therapeutic Patents 2000; 10 (5): 575-600.

17. Supuran CT. Carbonic anhydrases: novel therapeutic applications for inhibitors and activators. Nature reviews Drug Discovery 2008; 7 (2): 168-181.

18. Yiğit M, Yiğit B, Taslimi P, Özdemir İ, Karaman M et al. Novel amine-functionalized benzimidazolium salts: Synthesis, characterization, bioactivity, and molecular docking studies. Journal of Molecular Structure 2020; 1207: 127802.

19. Nowakowska Z. A review of anti-infective and anti-inflammatory chalcones. European Journal of Medicinal Chemistry 2007; 42 (2): 125-137.

20. Gafner S, Wolfender J-L, Mavi S, Hostettmann K. Antifungal and antibacterial chalcones from Myrica serrata. Planta Medica 1996; 62 (01): 67-69.

21. Mete E, Gul HI, Bilginer S, Algul O, Topaloglu ME et al. Synthesis and Antifungal Evaluation of 1-Aryl-2-dimethyl-aminomethyl-2-propen-1-one Hydrochlorides. Molecules 2011; 16 (6): 4660-4671.

22. Liu M, Wilairat P, Croft SL, Tan AL-C, Go M-L. Structure–activity relationships of antileishmanial and antimalarial chalcones. Bioorganic & Medicinal Chemistry 2003; 11 (13): 2729-2738.

23. Gopinathan A, Moidu M, Mukundan M, Ellickal Narayanan S, Narayanan H et al. Design, synthesis and biological evaluation of several aromatic substituted chalcones as antimalarial agents. Drug Development Research 2020.

24. Al-Saheb R, Makharza S, Al-Battah F, Abu-El-Halawa R, Kaimari T et al. Synthesis of new pyrazolone and pyrazole-based adamantyl chalcones and antimicrobial activity. Bioscience Reports 2020; 40 (9).

25. Bilginer S, Gul HI, Mete E, Das U, Sakagami H et al. 1-(3-Aminomethyl-4-hydroxyphenyl)-3-pyridinyl-2-propen-1-ones: a novel group of tumour-selective cytotoxins. Journal of Enzyme Inhibition and Medicinal Chemistry 2013; 28 (5): 974-980.

26. Burmaoglu S, Ozcan S, Balcioglu S, Gencel M, Noma SAA et al. Synthesis, biological evaluation and molecular docking studies of bis-chalcone derivatives as xanthine oxidase inhibitors and anticancer agents. Bioorganic Chemistry 2019; 91: 103149.

27. Bilginer S, Gul HI, Erdal FS, Sakagami H, Levent S et al. Synthesis, cytotoxicities, and carbonic anhydrase inhibition potential of 6-(3-aryl-2-propenoyl)-2 (3H)-benzoxazolones. Journal of Enzyme Inhibition and Medicinal Chemistry 2019; 34 (1): 1722-1729.

28. Sivakumar P, Prabhakar P, Doble M. Synthesis, antioxidant evaluation, and quantitative structure–activity relationship studies of chalcones. Medicinal Chemistry Research 2011; 20 (4): 482-492.

29. Prabakaran G, Manivarman S, Bharanidharan M. Catalytic synthesis, ADMET, QSAR and molecular modeling studies of novel chalcone derivatives as highly potent antioxidant agents. Materials Today Proceedings (in press).

30. Bilginer S, Unluer E, Gul HI, Mete E, Isik S et al. Carbonic anhydrase inhibitors. Phenols incorporating 2-or 3-pyridyl-ethenylcarbonyl and tertiary amine moieties strongly inhibit Saccharomyces cerevisiae β-carbonic anhydrase. Journal of Enzyme Inhibition and Medicinal Chemistry 2014; 29 (4): 495-499.

31. Koçyiğit ÜM, Gezegen H, Taslimi P. Synthesis, characterization, and biological studies of chalcone derivatives containing Schiff bases: Synthetic derivatives for the treatment of epilepsy and Alzheimer's disease. Archiv der Pharmazie 2020: e2000202.

32. Burmaoglu S, Yilmaz AO, Polat MF, Kaya R, Gulcin I et al. Synthesis and biological evaluation of novel tris-chalcones as potent carbonic anhydrase, acetylcholinesterase, butyrylcholinesterase and α-glycosidase inhibitors. Bioorganic Chemistry 2019; 85: 191-197.

33. Liu H-R, Liu X-J, Fan H-Q, Tang J-J, Gao X-H et al. Design, synthesis and pharmacological evaluation of chalcone derivatives as acetylcholinesterase inhibitors. Bioorganic & Medicinal Chemistry 2014; 22 (21): 6124-6133.

34. Riswanto FDO, Hariono M, Yuliani SH, Istyastono EP. Computer-aided design of chalcone derivatives as lead compounds targeting acetylcholinesterase. Indonesian Journal of Pharmacy 2017; 28 (2): 100.

35. Hsieh C-T, Hsieh T-J, El-Shazly M, Chuang D-W, Tsai Y-H et al. Synthesis of chalcone derivatives as potential anti-diabetic agents. Bioorganic & Medicinal Chemistry Letters 2012; 22 (12): 3912-3915.

36. Chinthala Y, Thakur S, Tirunagari S, Chinde S, Domatti AK et al. Synthesis, docking and ADMET studies of novel chalcone triazoles for anti-cancer and anti-diabetic activity. European Journal of Medicinal Chemistry 2015; 93: 564-573.

37. Petrov OI, Ivanova YB, Gerova MS, Momekov GT. Synthesis and cytotoxicity of new Mannich bases of 6-[3-(3, 4, 5-Trimetoxyphenyl)-2-propenoyl]-2 (3H)-benzoxazolone. Letters in Drug Design & Discovery 2020; 17 (4): 512-517.

38. Guo Y, Bao C, Li F, Hou E, Qin S et al. Discovery, synthesis, and biological evaluation of dunnianol-based mannich bases against methicillin-resistant staphylococcus aureus (MRSA). ACS Infectious Diseases 2020; 6 (9): 2478-2489.

39. Marinescu M, Cinteză LO, Marton GI, Chifiriuc M-C, Popa M et al. Synthesis, density functional theory study and in vitro antimicrobial evaluation of new benzimidazole Mannich bases. BMC Chemistry 2020; 14 (1): 1-16.

40. Dascalu A-E, Ghinet A, Lipka E, Furman C, Rigo B et al. Design, synthesis and antifungal activity of pterolactam-inspired amide Mannich bases. Fitoterapia 2020: 104581.

41. Ozgun DO, Yamali C, Gul HI, Taslimi P, Gulcin I et al. Inhibitory effects of isatin Mannich bases on carbonic anhydrases, acetylcholinesterase, and butyrylcholinesterase. Journal of Enzyme Inhibition and Medicinal Chemistry 2016; 31 (6): 1498-1501.

42. I Gul H, Demirtas A, Ucar G, Taslimi P, Gulcin I. Synthesis of Mannich bases by two different methods and evaluation of their acetylcholine esterase and carbonic anhydrase inhibitory activities. Letters in Drug Design & Discovery 2017; 14 (5): 573-580.

43. Sieger GM, Barringer WC, Krueger JE. Mannich derivatives of medicinals. 2. Derivatives of some carbonic anhydrase inhibitors. Journal of Medicinal Chemistry 1971; 14 (5): 458-460.

44. Büyükkıdan N, Büyükkıdan B, Bülbül M, Özer S, Gonca Yalçın H. Synthesis and characterization of phenolic Mannich bases and effects of these compounds on human carbonic anhydrase isozymes I and II. Journal of Enzyme Inhibition and Medicinal Chemistry 2013; 28 (2): 337-342.

45. Duan K, Liu H, Fan H, Zhang J, Wang Q. Synthesis and anticholinesterase inhibitory activity of Mannich base derivatives of flavonoids. Journal of Chemical Research 2014; 38 (7): 443-446.

46. Soyer Z, Parlar S, Alptuzun V. Synthesis and acetylcholinesterase (AChE) inhibitory activity of some N-substituted-5-chloro-2 (3H)-benzoxazolone derivatives. Marmara Pharmaceutical Journal 2013; 17 (1): 15-20.

47. M Huttunen K, Rautio J. Prodrugs-an efficient way to breach delivery and targeting barriers. Current Topics in Medicinal Chemistry 2011; 11 (18): 2265-2287.

48. Roman G. Mannich bases in medicinal chemistry and drug design. European Journal of Medicinal Chemistry 2015; 89: 743-816.

49. Yamali C, Tugrak M, Gul HI, Tanc M, Supuran CT. The inhibitory effects of phenolic Mannich bases on carbonic anhydrase I and II isoenzymes. Journal of Enzyme Inhibition and Medicinal Chemistry 2016; 31 (6): 1678-1681.

50. Ivanova Y, Momekov G, Petrov O, Karaivanova M, Kalcheva V. Cytotoxic Mannich bases of 6-(3-aryl-2-propenoyl)-2 (3H)-benzoxazolones. European Journal of Medicinal Chemistry 2007; 42 (11-12): 1382-1387.

51. Kucukoglu K, Gul HI, Taslimi P, Gulcin I, Supuran CT. Investigation of inhibitory properties of some hydrazone compounds on hCA I, hCA II and AChE enzymes. Bioorganic Chemistry 2019; 86: 316-321.

52. Yamali C, Gul HI, Ece A, Taslimi P, Gulcin I. Synthesis, molecular modeling, and biological evaluation of 4-[5-aryl-3-(thiophen-2-yl)-4, 5-dihydro-1H-pyrazol-1-yl] benzenesulfonamides toward acetylcholinesterase, carbonic anhydrase I and II enzymes. Chemical biology & Drug Design 2018; 91 (4): 854-866.

53. Ozgun DO, Gul HI, Yamali C, Sakagami H, Gulcin I et al. Synthesis and bioactivities of pyrazoline benzensulfonamides as carbonic anhydrase and acetylcholinesterase inhibitors with low cytotoxicity. Bioorganic Chemistry 2019; 84: 511-517.

54. Gul HI, Demirtas A, Ucar G, Taslimi P, Gulcin I. Synthesis of Mannich bases by two different methods and evaluation of their acetylcholine esterase and carbonic anhydrase inhibitory activities. Letters in Drug Design & Discovery 2017; 14 (5): 573-580.

55. Yamali C, Gul HI, Kazaz C, Levent S, Gulcin I. Synthesis, structure elucidation, and in vitro pharmacological evaluation of novel polyfluoro substituted pyrazoline type sulfonamides as multi-target agents for inhibition of acetylcholinesterase and carbonic anhydrase I and II enzymes. Bioorganic Chemistry 2020; 96: 103627.

56. Ellman GL, Courtney KD, Andres Jr V, Featherstone RM. A new and rapid colorimetric determination of acetylcholinesterase activity. Biochemical Pharmacology 1961; 7 (2): 88-95.

57. Mamedova G, Mahmudova A, Mamedov S, Erden Y, Taslimi P et al. Novel tribenzylaminobenzolsulphonylimine based on their pyrazine and pyridazines: Synthesis, characterization, antidiabetic, anticancer, anticholinergic, and molecular docking studies. Bioorganic Chemistry 2019; 93: 103313.

58. Gulcin I, Kaya R, Goren AC, Akincioglu H, Topal M et al. Anticholinergic, antidiabetic and antioxidant activities of Cinnamon (Cinnamomum verum) bark extracts: polyphenol contents analysis by LC-MS/MS. International Journal of Food Properties 2019; 22 (1): 1511-1526.

59. Taslimi P, Türkan F, Cetin A, Burhan H, Karaman M et al. Pyrazole [3, 4-d] pyridazine derivatives: Molecular docking and explore of acetylcholinesterase and carbonic anhydrase enzymes inhibitors as anticholinergics potentials. Bioorganic Chemistry 2019; 92: 103213.

60. Bilginer S, Gonder B, Gul HI, Kaya R, Gulcin I et al. Novel sulphonamides incorporating triazene moieties show powerful carbonic anhydrase I and II inhibitory properties. Journal of Enzyme Inhibition and Medicinal Chemistry 2020; 35 (1): 325-329.

61. Gul HI, Tugrak M, Gul M, Mazlumoglu S, Sakagami H et al. New phenolic Mannich bases with piperazines and their bioactivities. Bioorganic Chemistry 2019; 90: 103057.

62. Gul HI, Yamali C, Bulbuller M, Kirmizibayrak PB, Gul M et al. Anticancer effects of new dibenzenesulfonamides by inducing apoptosis and autophagy pathways and their carbonic anhydrase inhibitory effects on hCA I, hCA II, hCA IX, hCA XII isoenzymes. Bioorganic Chemistry 2018; 78: 290-297.

63. Tugrak M, Gul HI, Bandow K, Sakagami H, Gulcin I et al. Synthesis and biological evaluation of some new mono Mannich bases with piperazines as possible anticancer agents and carbonic anhydrase inhibitors. Bioorganic Chemistry 2019; 90: 103095.

64. Mete E, Comez B, Inci Gul H, Gulcin I, Supuran CT. Synthesis and carbonic anhydrase inhibitory activities of new thienyl-substituted pyrazoline benzenesulfonamides. Journal of Enzyme Inhibition and Medicinal Chemistry 2016; 31 (sup2): 1-5.

65. Yıldırım A, Atmaca U, Keskin A, Topal M, Celik M et al. N-Acylsulfonamides strongly inhibit human carbonic anhydrase isoenzymes I and II. Bioorganic & Medicinal Chemistry 2015; 23 (10): 2598-2605.

66. Akıncıoğlu A, Akbaba Y, Göçer H, Göksu S, Gülçin İ et al. Novel sulfamides as potential carbonic anhydrase isoenzymes inhibitors. Bioorganic & Medicinal Chemistry 2013; 21 (6): 1379-1385.

67. Aksu K, Nar M, Tanc M, Vullo D, Gülçin İ et al. Synthesis and carbonic anhydrase inhibitory properties of sulfamides structurally related to dopamine. Bioorganic & Medicinal Chemistry 2013; 21 (11): 2925-2931.

68. Boztas M, Cetinkaya Y, Topal M, Gulcin I, Menzek A et al. Synthesis and carbonic anhydrase isoenzymes I, II, IX, and XII inhibitory effects of dimethoxybromophenol derivatives incorporating cyclopropane moieties. Journal of Medicinal Chemistry 2015; 58 (2): 640-650.

69. Scozzafava A, Passaponti M, Supuran CT, Gülçin İ. Carbonic anhydrase inhibitors: guaiacol and catechol derivatives effectively inhibit certain human carbonic anhydrase isoenzymes (hCA I, II, IX and XII). Journal of Enzyme Inhibition and Medicinal Chemistry 2015; 30 (4): 586-591.

70. Gocer H, Aslan A, Gülçin İ, Supuran CT. Spirobisnaphthalenes effectively inhibit carbonic anhydrase. Journal of Enzyme Inhibition and Medicinal Chemistry 2016; 31 (3): 503-507.

71. Bilginer S, Koca M. Synthesis, Cholinesterase inhibition and molecular docking studies of novel Mannich bases of banzoxazolone chalcone compounds. In: 8th International Drug Chemistry Conference; 27 February-1 March; Antalya/ Turkey 2020. p. 107-111.

72. Daina A, Michielin O, Zoete V. SwissADME: a free web tool to evaluate pharmacokinetics, drug-likeness and medicinal chemistry friendliness of small molecules. Scientific Reports 2017; 7: 42717.

73. Lipinski CA, Lombardo F, Dominy BW, Feeney PJ. Experimental and computational approaches to estimate solubility and permeability in drug discovery and development settings. Advanced Drug Delivery Reviews 1997; 23 (1-3): 3-25.